

The effect of Fe atoms on the adsorption of a W atom on W(100) surface

J. Houze,^{1,2} Sungho Kim,^{1,2} Seong-Jin Park,² Randall M. German,^{3,2}

M. F. Horstemeyer,^{3,2} and Seong-Gon Kim^{1,2,*}

¹ *Department of Physics and Astronomy,*

Mississippi State University, Mississippi State, MS 39762, USA

² *Center for Advanced Vehicular Systems,*

Mississippi State University, Mississippi State, MS 39762, USA

³ *Department of Mechanical Engineering,*

Mississippi State University, Mississippi State, MS 39762, USA

(Dated: November 1, 2018)

Abstract

We report a first-principles calculation that models the effect of iron (Fe) atoms on the adsorption of a tungsten (W) atom on W(100) surfaces. The adsorption of a W atom on a clean W(100) surface is compared with that of a W atom on a W(100) surface covered with a monolayer of Fe atoms. The total energy of the system is computed as the function of the height of the W adatom. Our result shows that the W atom first adsorbs on top of the Fe monolayer. Then the W atom can replace one of the Fe atoms through a path with a moderate energy barrier and reduce its energy further. This intermediate site makes the adsorption (and desorption) of W atoms a two-step process in the presence of Fe atoms and lowers the overall adsorption energy by nearly 2.4 eV. The Fe atoms also provide a surface for W atoms to adsorb facilitating the diffusion of W atoms. The combination of these two effects result in a much more efficient desorption and diffusion of W atoms in the presence of Fe atoms. Our result provides a fundamental mechanism that can explain the activated sintering of tungsten by Fe atoms.

PACS numbers: 68.43.-h, 68.43.Bc, 68.43.Fg, 81.20.Ev,

I. INTRODUCTION

The sintering of tungsten can be enhanced by the addition of small amounts of alloying elements (0.5-1.0%) from the iron group metals such as Fe, Co, and Ni. This phenomenon is called “activated sintering.”^{1,2} These additive species lower the activation energy for sintering, resulting in a much lower sintering temperature, shorter sintering time, or better properties.³ The classical theory explains this by the enhancement of grain-boundary diffusion in tungsten due to the presence of the respective element in the grain boundary. High densities (up to 99% of bulk) can be obtained even at 1100 °C (at this temperature, tungsten compacts are commonly presintered).^{3,4,5} Because of high melting point and large surface energy, tungsten has been considered to be one of the best substrates to grow thin magnetic films on and consequently its interaction with magnetic materials including Fe has been studied extensively.^{6,7}

In this study, we investigated the activated sintering of tungsten by iron from a quantum mechanics point of view. Adsorption and desorption are two of the main mechanisms of sintering. The aim of the present work is to explore the morphology and energetics of thin Fe layers on W surfaces and their effect on the adsorption/desorption of W atoms and eventually on the sintering of tungsten. Our approach is based on density functional theory and we show that our atomistic first-principles modeling and simulation can supplement the experiments and provide a fundamental mechanism of the activated sintering of tungsten by iron. Our present study is focused on the adsorption of tungsten on W(100) surfaces. The adsorption of W atoms on a clean W(100) surface is compared with the one on the same surface covered with a monolayer of Fe atoms. The surface morphology and energy barriers were calculated and analyzed to elucidate the role of Fe atoms in the adsorption of W atoms.

II. METHODS

The adsorption energy of a single adatom E_{ads} at height z is given by

$$E_{\text{ads}}(z) = E_{\text{tot}}(z) - E_{\text{tot}}(\infty) \quad (1)$$

where $E_{\text{tot}}(z)$ is the total energy of the structure with the adatom adsorbed at height z on the surface and $E_{\text{tot}}(\infty)$ is the total energy of the same surface with the adatom at an

infinite distance.

All *Ab initio* total-energy calculations and geometry optimizations are performed within density functional theory (DFT) using Blöchl’s all-electron projector augmented wave (PAW) method⁸ as implemented by Kresse et al.⁹ For the treatment of electron exchange and correlation, we use the generalized gradient approximation (GGA) of Perdew et al.¹⁰ The Kohn-Sham equations are solved using a preconditioned band-by-band conjugate-gradient (CG) minimization.¹¹ The plane-wave cutoff energy is set to at least 350 eV in all calculations. The tungsten lattice constant of 3.175 Å we obtained is slightly larger than the experimental value of 3.165 Å.¹² We use a standard supercell technique, modeling the W(100) surface with (3×3) surface unit cell by a slab consisting of seven substrate layers, separated by 10.0 Å of vacuum. Atoms in the bottom layer are fixed at their bulk positions, while all other atoms are allowed to relax until the root-mean-square (rms) force is less than 0.001 eV/Å. The Brillouin zone is sampled with a density equivalent to at least 81 *k*-points in (1×1) surface Brillouin zone using the Monkhorst-Pack scheme.¹³ A Fermi-level smearing of 0.2 eV was applied using the Methfessel-Paxton method.¹⁴

III. RESULTS AND DISCUSSION

In this study, we focus on the adsorption of W atoms on W(100) and Fe/W(100) surfaces. Fig. 1 shows the optimized structures of adsorbed W atoms in different configurations. In Fig. 1(A), a W adatom is adsorbed on a clean W(100) surface, while Fig. 1(B-D) show three different configurations of a W adatom adsorbed on W(100) surface covered by a Fe monolayer. For each configuration, all atoms are fully relaxed except the atoms in the bottom layer.

W(100) surface is known to exhibit a $(\sqrt{2}\times\sqrt{2})R45^\circ$ reconstruction at low temperatures.¹⁵ It also has been observed that the surface reconstruction vanishes locally upon the adsorption of a Mn atom on W(100) surface.⁷ Our result is in good agreement with these observations. Two deltoids in Fig. 1(A) show the distortion of nearest neighbor bond angles due to surface reconstruction. The upper-left deltoid containing the W adatom is indistinguishable from a square reflecting the fact that the reconstruction is suppressed due to the adsorption of the W atom. On the contrary, the lower-right deltoid has two equal obtuse angles of 96.1° indicating the distortion of bond angles due to surface reconstruction. However, because the

deltoid is adjacent to the W adatom adsorption site, the angle is smaller than 106° observed for clean W(100) surfaces.⁶

The adsorption energies and the optimized height for these configurations are listed in Table I. Fig. 2 also shows the adsorption energy of a W adatom on two different surfaces, a clean W(100) surface and an Fe monolayer on W(100) surface, as a function of the height. For the configurations (A-D), only the bottom layers are fixed and all other atom positions are fully relaxed. The other points in Fig. 2 are generated by additionally fixing the height of the W adatom.

Fig. 1(B) shows the morphology of a W atom adsorbed on an Fe monolayer on the W(100) surface. It turned out that the most energetically favorable adsorption site for a W adatom is not directly above the center of the square formed by four neighboring Fe atoms, but closer to one of the surrounding Fe atoms. In Fig. 1(C), the W adatom is pushed in toward the closest Fe atom. Consequently, the Fe atom is displaced from its place and forms a horizontal dimer with the W adatom. Although configuration *C* has a higher adsorption energy than that of configuration *B* by $E_C - E_B = 0.53$ eV as shown in Table I, configuration *C* is stable against small perturbation of atomic positions of the W-Fe dimer. When the W adatom is pushed in further, it replaces the Fe atom completely and the displaced Fe atom will adsorb above the Fe monolayer, as shown as configuration *D* in Fig. 1(D).

Our result is consistent with the experimental observation that the addition of a small amount of Fe atoms enhances the sintering of tungsten. Our study shows that there are two main effects of Fe atoms on tungsten sintering. First, the existence of a stable adsorption site on an Fe monolayer (configuration *B*) leads to more efficient desorption of W atoms. This means that the desorption of W atoms occurs in two stages when Fe atoms are present. Starting from configuration *D*, W atoms first move to configuration *B* by passing through the Fe layers via the pathway $D \rightarrow C \rightarrow B$. The W atoms overcome a moderate size energy barrier of $E_C - E_D = 0.99$ eV utilizing the thermal excitation readily available during sintering process. At the second stage, W atoms can be desorbed from configuration *B*. Compared to the direct desorption from configuration *A* in the absence of Fe atoms, this multi-stage desorption through configuration *B* is much more efficient because the adsorption energy of W atom at *B* is significantly lower than at *A*: $E_B - E_A = (E_B - E_D) + (E_D - E_A) = 0.46 + 1.93 = 2.39$ eV (See Table I). Second, the existence of stable adsorption sites on Fe monolayer makes the diffusion of W atoms on Fe atoms available for an efficient sintering

process. The smaller adsorption energy of a W atom on an Fe monolayer strongly suggests that the Fe thin film layer will provide a much smoother platform for the adsorbed W atoms to diffuse. This enhanced diffusion will facilitate the movement of W atoms from one place to another. A further detailed investigation will be required to elucidate the effect of Fe atoms on diffusion of W atoms and it will be reported elsewhere. Comparison with different activation agents, such as Co or Ni, will also provide valuable information in validating the mechanism proposed from the present work.

IV. CONCLUSIONS

We have presented a first-principles DFT investigation of the structure and energetics of a W adatom on W(100) and Fe/W(100) surfaces. We found that W atoms adsorb on an Fe monolayer. Fe atoms also reduce the adsorption energy of W adatoms on W(100) surface substantially. Fe thin film layers also allow W atoms to pass through easily and thus facilitate the diffusion of W atoms.

V. ACKNOWLEDGMENT

The authors are grateful to the Center for Advanced Vehicular Systems at Mississippi State University for supporting this study. Computer time allocation has been provided by the High Performance Computing Collaboratory (HPC²) at Mississippi State University.

* Electronic address: kimsg@ccs.msstate.edu

¹ J. H. Brophy, H. W. Hayden, and J. Wulff, *Trans. TMS-AIME* **221**, 1225 (1961).

² R. M. German and Z. A. Munir, *High Temp. Sci.* **8**, 267 (1976).

³ R. M. German, *Powder Metallurgy & Particular Materials Processing* (Metal Powder Industrial Federation, Princeton, NJ, 2005).

⁴ V. V. Panichkina, *Powder Metallurgy and Metal Ceramics* **6**, 87 (1967).

⁵ G. V. Samsonov and V. I. Yakovlev, *Powder Metallurgy and Metal Ceramics* **8**, 804 (1969).

⁶ S. Denmler and J. Hafner, *Physical Review B (Condensed Matter and Materials Physics)* **72**, 214413 (pages 17) (2005).

- ⁷ D. Spisak and J. Hafner, Physical Review B (Condensed Matter and Materials Physics) **70**, 195426 (pages 13) (2004).
- ⁸ P. E. Blöchl, Phys. Rev. B **50**, 17953 (1994).
- ⁹ G. Kresse and D. Joubert, Phys. Rev. B **59**, 1758 (1999).
- ¹⁰ J. P. Perdew, K. Burke, and M. Ernzerhof, Phys. Rev. Lett. **77**, 3865 (1996).
- ¹¹ G. Kresse and J. Hafner, Phys. Rev. B **47**, 558 (1993).
- ¹² *American Institute of Physics Handbook* (McGraw-Hill, New York, 1972).
- ¹³ H. J. Monkhorst and J. D. Pack, Phys. Rev. B **13**, 5188 (1976).
- ¹⁴ M. Methfessel and A. T. Paxton, Phys. Rev. B **40**, 3616 (1989).
- ¹⁵ M. S. Altman, P. J. Estrup, and I. K. Robinson, Phys. Rev. B **38**, 5211 (1988).

TABLE I: The adsorption energy E_{ads} and the optimized height z for different configurations in Fig. 1. Energy differences between different configurations are also listed.

Config.	E_{ads} (eV)	z (Å)	ΔE (eV)
A	-11.38	1.41	$E_{\text{D}} - E_{\text{A}} = 1.93$
D	-9.45	1.38	$E_{\text{C}} - E_{\text{D}} = 0.99$
C	-8.46	1.82	$E_{\text{B}} - E_{\text{C}} = -0.53$
B	-8.99	2.18	$E_{\text{B}} - E_{\text{D}} = 0.46$

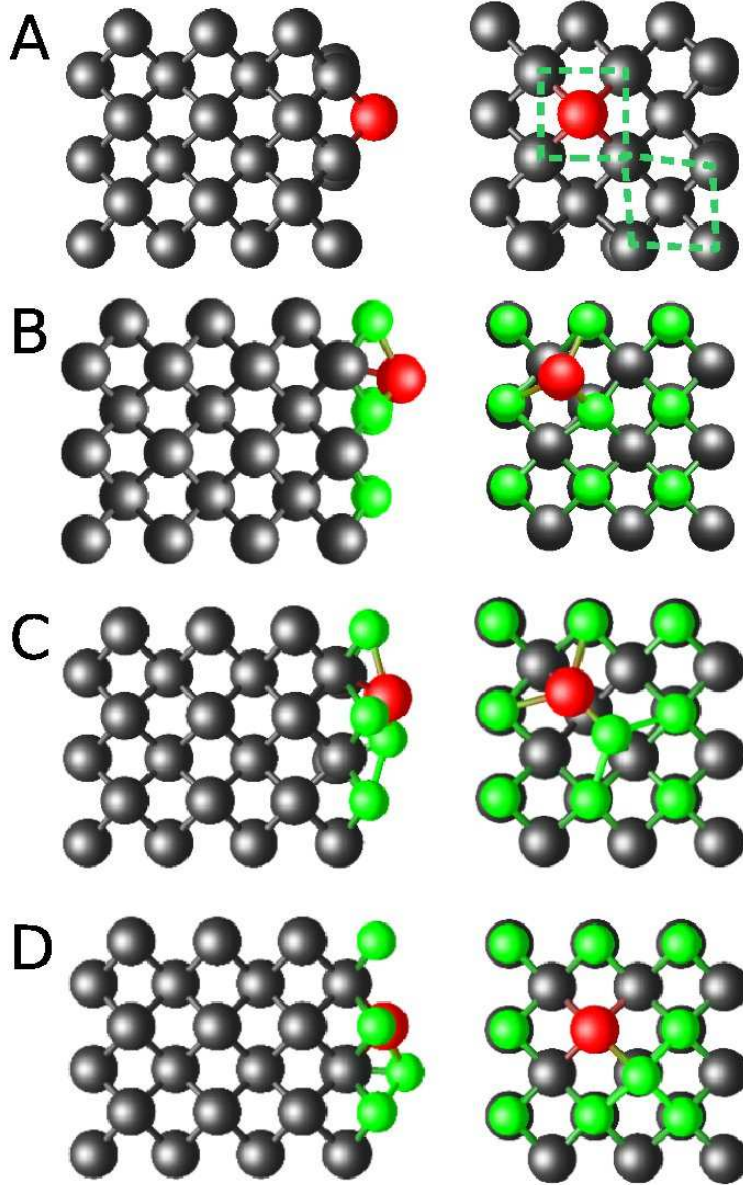


FIG. 1: (color online) Adsorption of W on (A) clean W(100) and (B-D) Fe monolayer on W(100) surfaces. The side views (left column) and top views (right column) are given. (3×3) surface unit cells are used for our calculations as shown in top views. Black spheres represent W atoms in the substrate layers while a red sphere represents the W adatom. Fe atoms are represented by smaller green spheres. (A) W adatom is adsorbed on a clean W(100) surface. (B) W adatom is adsorbed on a Fe monolayer covering W(100) surface. (C) W adatom is pushed in toward the closest Fe atom, which is displaced from its place. The W and Fe atoms form a dimer that is parallel to W(100) surface. (D) W adatom completely replaced the Fe atom and the displaced Fe atom is now adsorbed on the Fe monolayer. Two deltoids in (A) show the distortion of nearest neighbor W atoms bonds due to surface reconstruction.

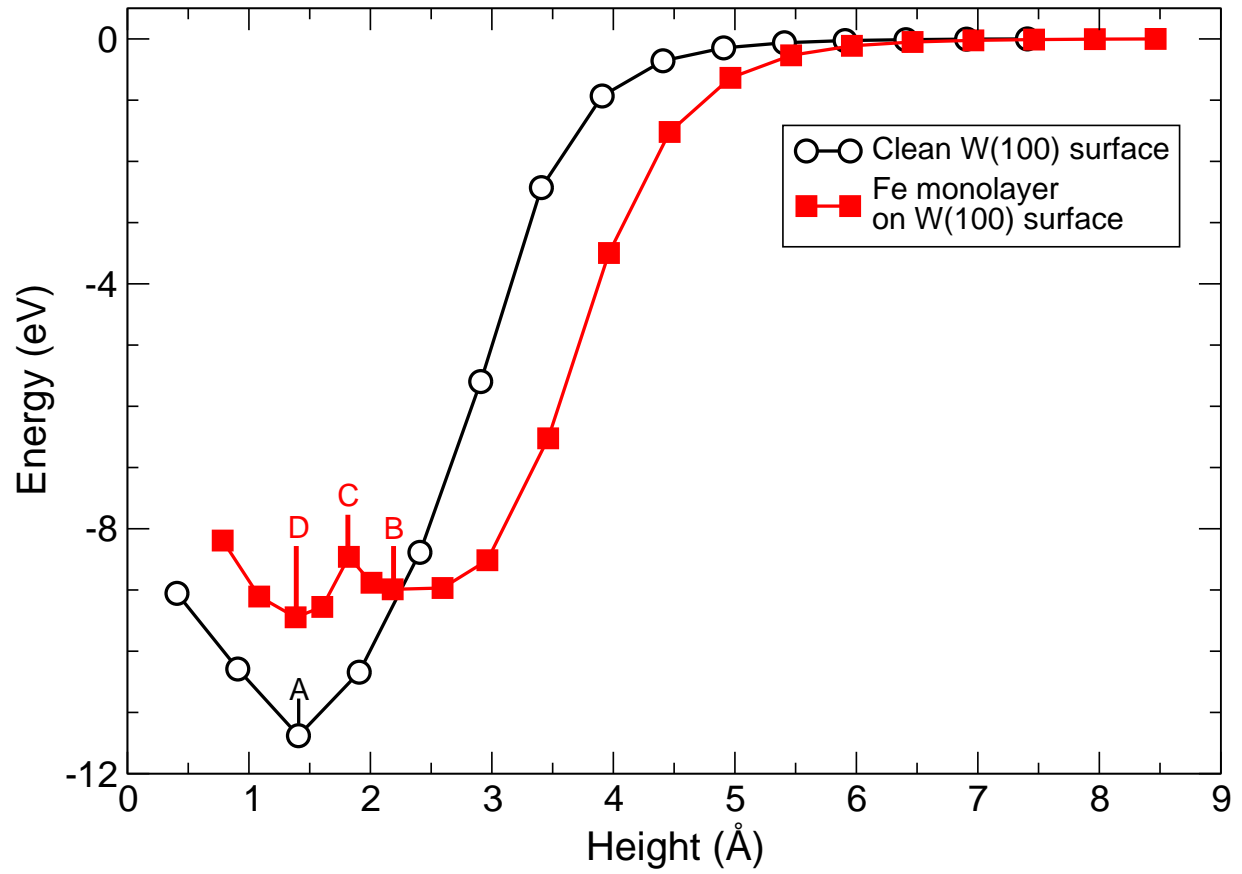


FIG. 2: (color online) The adsorption energy $E_{\text{ads}}(z)$ of a W adatom on a clean W(100) surface (black open circles) and on a Fe monolayer on W(100) surface (red filled squares). The height of W adatom z is measured from the W atoms in the top layer of W(100) surface.